Scanning-tunneling-microscopy investigation of the nucleation and growth of Ag/Si(111)-($\sqrt{3}\times\sqrt{3}$)

D. W. McComb, D. J. Moffatt, and P. A. Hackett
Steacie Institute for Molecular Sciences, National Research Council of Canada, 100 Sussex Drive, Ottawa, Ontario, Canada K1A 0R6

B. R. Williams and B. F. Mason
Institute for Microstructural Sciences, National Research Council of Canada, Montreal Road, Ottawa, Ontario, Canada K1A OR6
(Received 21 December 1993)

The scanning tunneling microscope has been used to identify and distinguish between various stages of reactive growth of Ag on Si(111)-(7×7) at 450 °C. Continuous investigation of the reaction trend was made possible by producing a concentration gradient of Ag on the substrate. The surface features observed, such as hole-island pairs, are dependent on the sample coverage. Mechanisms for the formation of Ag/Si(111)-($\sqrt{3}\times\sqrt{3}$) are proposed, and experimental confirmation of their validity is presented. Antiphase boundaries between neighboring ($\sqrt{3}\times\sqrt{3}$) domains have been observed, and a model for the atomic structure across such a boundary is shown. At near monolayer coverages small regions that exhibit the Si(111)-(1×1) structure have been identified.

I. INTRODUCTION

A process which has attracted considerable interest in recent years is the reactive growth of Ag on the Si(111)-(7×7) surface.[1-5] As a result of extensive studies using x-ray diffraction, electron diffraction, ion scattering, and scanning tunneling microscopy (STM), the chemistry of the interaction between Ag and Si(111) is currently described as follows: from room temperature to 200 °C, deposited Ag migrates and nucleates to grow as three-dimensional bulklike structures; between 200 and 500 °C, there is sufficient activation energy to cause reactive growth of Ag to form the ($\sqrt{3}\times\sqrt{3}$) structure; and, finally, above 500 °C, progressive desorption of Ag occurs, and if the silicon crystal is subsequently flashed to 1200 °C, clean Si(111)-(7×7) results. A more complex phase diagram which includes the effect of annealing the ($\sqrt{3}\times\sqrt{3}$) structures has been recently obtained from STM investigations.[13] The structure of the ($\sqrt{3}\times\sqrt{3}$) unit cell, which remains open to question, is consistent with the honeycomb-chain-trimer (HCT) model.[6] It has been suggested that one mode of the restructuring of the silicon surface from (7×7) to ($\sqrt{3}\times\sqrt{3}$) in the presence of Ag occurs via a growth process described as hole-island pair formation.[7,8] The mechanism proposed is that Ag atoms deposited on a terrace react with the Si surface to form a ($\sqrt{3}\times\sqrt{3}$) hole, which is below the level of the (7×7) adatoms. Si atoms are thought to be ejected from the hole region and react with migrating Ag atoms to form a ($\sqrt{3}\times\sqrt{3}$) island, at a level above the (7×7) surface, in the neighborhood of the hole. If the coverage of silver is too low, hole-island pairs do not form on the (7×7) terraces, and instead ($\sqrt{3}\times\sqrt{3}$) domains are observed at step edges.[8] This observation has not been thoroughly investigated, and in this paper will show that conditions exist where the two types of ($\sqrt{3}\times\sqrt{3}$) domains can be present on the surface. We will demonstrate that the Ag atoms diffuse readily across (7×7) terraces to the step edges at low coverages, and it is only above a critical coverage on a particular terrace that hole-island pair formation commences on that terrace. The parameters which determine the coverage at which this growth mode transition occurs will be identified and discussed. A number of mechanisms for the growth of the two types of ($\sqrt{3}\times\sqrt{3}$) domains will also be considered. The ratio of the area of the holes to that of the island has been identified as one parameter, which provides insight into the structure of the hole-island pair. Although this ratio has been reported to be constant,[5,13] we will show that it is dependent on the coverage. This study will contribute to the structural knowledge of the ($\sqrt{3}\times\sqrt{3}$) phase by demonstrating the existence of many antiphase boundaries, which develop on growth, between ($\sqrt{3}\times\sqrt{3}$) domains. The detailed atomic structure across this boundary will be considered. In addition, the presence of small regions of Si(111)-(1×1) between ($\sqrt{3}\times\sqrt{3}$) domains at close to monolayer coverage will be demonstrated.

II. EXPERIMENT

Experiments were conducted in UHV ($P=3\times10^{-11}$ torr) using a commercially available scanning tunneling microscope.[9] Low-energy electron diffraction (LEED) and Auger electron spectroscopy (AES) facilities were also available in the UHV chamber. Samples of Si(111) were degassed in vacuum at 850 °C, and were cleaned by flash annealing to 1200 °C. LEED, AES, and STM were used to monitor the quality of the Si(111)-(7×7) surface produced. Ag was deposited onto the surface at a sample temperature of 450 °C from an evaporation source consisting of fused Ag pellets in a Mo basket. The Ag source was enclosed in a small metal cylinder with a rectangular nozzle. By directing the effusion beam at an angle to the substrate a gradual change in the concentration of silver across the sample could be obtained. This enables continuous investigation of the coverage-dependent features of the metal overlayer growth. Other specific experi-

ments were carried out at fixed coverages. AES was used at all experimental stages to monitor the chemical purity of the surface, and contamination was below the detectable limits at all stages. The Ag flux was not measured, but an estimate of the coverage of Ag on the substrate was obtained directly from the scanning tunneling microscope images. The tunneling current and sample bias used for acquisition of the scanning tunneling microscope images are given in the figure captions. No image processing of the experimental data was performed except where, as indicated in the text, it was necessary to adjust the contrast range in the image.

III. RESULTS AND DISCUSSION

LEED patterns from the sample with a concentration gradient are shown in Fig. 1. It is clear that on the right-hand side of the sample the diffraction pattern is due solely to the $(\sqrt{3}\times\sqrt{3})$ adsorbed phase, suggesting that close to monolayer coverage has been obtained. Progressive patterns obtained towards the left-hand side show a gradual increase in the intensity of diffraction spots associated with the (7×7) silicon surface. On the far left there is little observed contribution to the LEED pattern from the $(\sqrt{3}\times\sqrt{3})$ Ag structure. In this manner, strong evidence for the presence of a concentration gradient of Ag on the Si(111) surface is obtained prior to STM investigations.

As noted above, the Ag $(\sqrt{3}\times\sqrt{3})$ structure is stable between $\sim$200–500 °C. By heating to 600 °C the Ag atoms can be desorbed from the Si(111) surface, and if the crystal is subsequently flash annealed to 1200 °C, a clean (7×7) surface is recovered. However, the formation of the $(\sqrt{3}\times\sqrt{3})$ structure on Si(111) and its subsequent desorption can be considered to be a surface-etching process. We have found that the Si(111)-(7×7) surface recovered after reaction and desorption shows a modification, which is manifested by a higher than normal incidence of surface steps, which are more than a single step in height. This phenomenon has not been reported to date, and is not completely understood. We note below that the growth behavior of the $(\sqrt{3}\times\sqrt{3})$ phase is modified by the presence of these multiple steps. The mechanism which leads to multiple steps probably has its origin in the height variation of the $(\sqrt{3}\times\sqrt{3})$ domains on the silicon surface, which result in nucleation of multiple height steps following desorption and flash annealing. The number of multiple steps on the samples used in this work varied considerably, but in general was significantly greater than those found on a freshly prepared Si(111) surface that had never undergone reaction with Ag atoms.

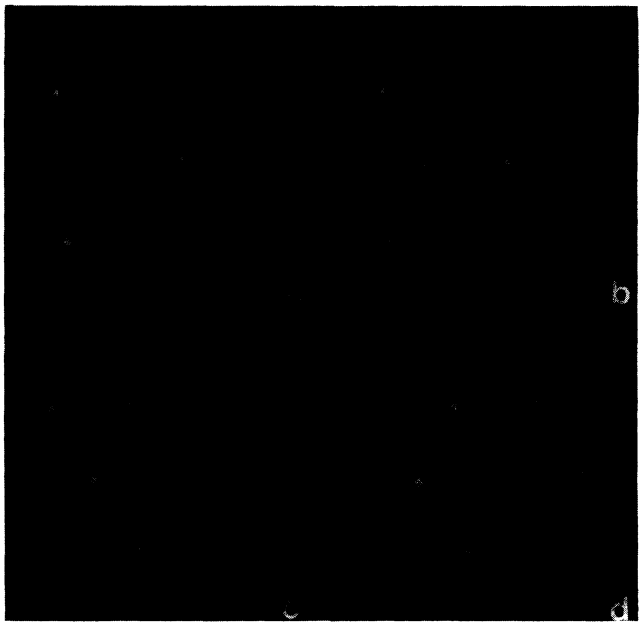

FIG. 1. LEED patterns showing an Ag $(\sqrt{3}\times\sqrt{3})$ concentration gradient on Si(111). The diffraction patterns were recorded with a beam energy of 38 eV. Patterns recorded at the left-hand side of the crystal, (a), only show spots associated with Si(111)-(7×7). As the sample is traversed, (b) and (c), the intensity of the spots due to the $(\sqrt{3}\times\sqrt{3})$ structure increases, until at the right-hand side, (d), only the diffraction pattern due to $(\sqrt{3}\times\sqrt{3})$ is apparent.

A. Reaction at the step edges

STM investigations of this surface reaction confirm the trend shown in LEED observations and provide added insight into the nucleation and growth of the metal overlayer. At the lowest coverages, large terraces of (7×7) are observed, which are unaltered by the exposure to Ag atoms. The presence of Ag is detected only at the step edge, where small domains exhibit the $(\sqrt{3}\times\sqrt{3})$ structure [Fig. 2(a)]. The interface between the (7×7) and the $(\sqrt{3}\times\sqrt{3})$ structures can be imaged with atomic resolution [Fig. 2(b)], to show that the $(\sqrt{3}\times\sqrt{3})$ structure is consistent with previously reported images,[1–3,5] and that the (7×7) structure is unaffected by the adjacent $(\sqrt{3}\times\sqrt{3})$ domain. It has been reported that the measured step height between $(\sqrt{3}\times\sqrt{3})$ and (7×7) domains is dependent on the bias conditions used in the STM.[5] In images of the filled states of the sample, the step up from regions of (7×7) to regions of $(\sqrt{3}\times\sqrt{3})$ is reported to vary from 1.9 to 1.2 Å, while the corresponding step down from (7×7) to $(\sqrt{3}\times\sqrt{3})$ ranges in height from 1.2 to 1.8 Å as the sample voltage is varied from -2.5 to -1.2 V.[5] Thus, despite the variation in step height, each type of step can be unambiguously determined in images of the filled states. Extensive studies of the voltage dependence of the step height are not pursued here, although we note that such measurements are also sensitive to the condition of the scanning tunneling microscope tip. However, for the image shown in Fig. 2(a), the $(\sqrt{3}\times\sqrt{3})$ domains at a monatomic step are approximately 1 Å above the lower terrace and 3 Å below the upper terrace. At these coverages the domains appear at the steps and are well separated from each other. Further, the domain edges, or reaction front, generally appear curved, with some evidence of faceting along both the $\langle 110\rangle$ and $\langle 11\bar{2}\rangle$ directions. At slightly higher coverage Ag continues to diffuse to the step edge, but reaction occurs in the (111) basal plane in regions adjacent to

the $(\sqrt{3}\times\sqrt{3})$ step edge. This is also illustrated in Fig. 2(a), where the confluence of steps in the bottom right-hand corner of the image has resulted in a larger local concentration of mobile Ag atoms. This effect will be discussed in detail later; however, the result is that the $(\sqrt{3}\times\sqrt{3})$ domains in this region have lower regions associated with them, within which the $(\sqrt{3}\times\sqrt{3})$ structure also exists. For the particular case shown, the lower, or hole region is approximately 4 Å below the height of the upper or island domain.

At a monatomic step the $(\sqrt{3}\times\sqrt{3})$ domains are generally curved in appearance on both fronts, although the step edge is generally straight, suggesting that growth has occurred away from the step edge on top of the lower terrace, as well as on the upper terrace, and on demarcation between the growth directions can be detected. In contrast, at steps which are more than one atomic layer high, the $(\sqrt{3}\times\sqrt{3})$ domain fronts are curved on one side with one edge of the domain defined by the step edge. This implies that the domains grow away from the step edge on either the upper or the lower terrace, but the growth does not cross the step edge [Fig. 2(a)]. A mechanism to explain this observation, based on the atom count approach used by Shibata and co-workers,[7,8] is illustrated schematically in Fig. 3. It is proposed that for reaction at a monatomic step, Ag atoms eject Si atoms from the surface layer of the upper terrace, and this free silicon diffuses to the lower terrace where it reacts with Ag atoms to continue the growth in this direction. Meanwhile, attack also continues on the upper terrace and, consequently, growth of the $(\sqrt{3}\times\sqrt{3})$ domain away from the step edge can occur in both directions. At a (7×7) step which is more than one unit high, a similar mechanism can be proposed, but the $(\sqrt{3}\times\sqrt{3})$ domains formed on the upper and the lower terraces are now at different heights, i.e., they are separated by one or more silicon bilayers. Thus, the $(\sqrt{3}\times\sqrt{3})$ structure can grow away from the step edge in either direction but cannot cross the step edge. In fact, many examples of adjacent $(\sqrt{3}\times\sqrt{3})$ domains which are separated by a multiple height step are observed, suggesting that silicon atoms ejected from the upper terrace do not rapidly diffuse away from their original locality before undergoing reaction with Ag atoms.

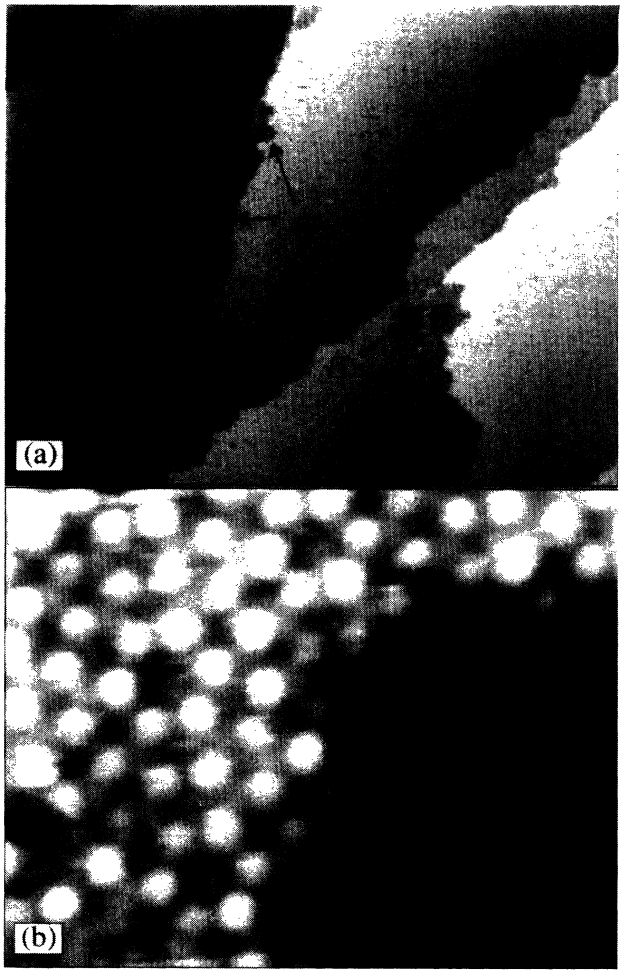

FIG. 2. (a) Image of the initial growth stage of Ag on Si(111) (1590×1270 Å^2, $I=1.2$ nA, $V=-0.9$ V). Isolated domains and bands of $(\sqrt{3}\times\sqrt{3})$ are apparent at the step edges. (b) Enlarged image of the interface between (7×7) and $(\sqrt{3}\times\sqrt{3})$.

Implicit to the mechanism described above is the diffusion of both Ag and Si atoms on the Si(111) surface. The barrier to diffusion for Ag on Si(111) is reported to be in the range 0.3–0.5 eV.[14] We are not aware of a value for the barrier to diffusion of Si on Si(111). However, it is established that cleaved Si(111)-(2×1) undergoes a phase transition to (7×7) at low temperatures (300–600 °C), which requires substantial rearrangement and diffusion of Si atoms, and implies that the barrier to diffusion must be small.[15] Thus, we can conclude that at 450 °C both Si and Ag will diffuse easily on Si(111).

Experimental confirmation of the proposed growth mode at monatomic steps, i.e., Si atom displacement from the upper terrace to the lower terrace, is obtained from

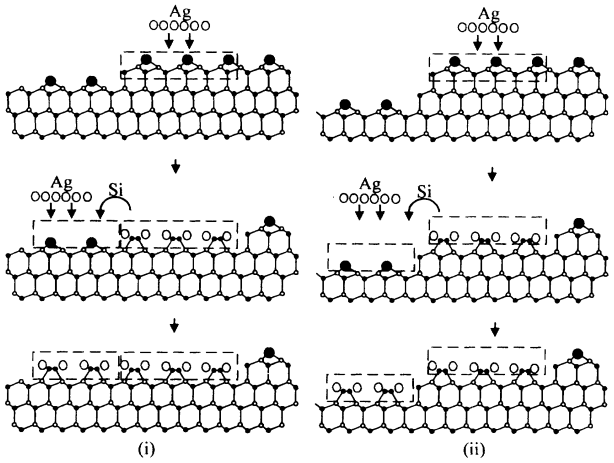

FIG. 3. Diagram detailing the mechanisms proposed for growth at single (i) and multiple (ii) height steps. For simplicity, the dimers and the stacking fault in the (7×7) unit cell are not shown. The silicon bilayers are represented by small filled and unfilled circles, the adatoms as large filled circles, and the Ag atoms as large unfilled circles. The silicon trimers formed are shown as pairs of small filled circles.

the image displayed in Fig. 4. A narrow band of $(\sqrt{3}\times\sqrt{3})$, which is about one-half of a (7×7) unit cell in width, in the $\langle 11\bar{2}\rangle$ direction, is observed at point *A*. This growth is terminated by the dimer rows of the unit cell, indicating that there could be a small barrier to subsequent reaction at this point. This band of $(\sqrt{3}\times\sqrt{3})$ can be viewed as the initial stage of growth at the step edge. Thus, the position of the band can be used as a marker for the step edge in the absence of reaction, and can be extrapolated (dashed line in Fig. 4) into regions where subsequent reaction has occurred. It is noted that a kink, which is half of a (7×7) unit cell in magnitude, exists in the narrow band of $(\sqrt{3}\times\sqrt{3})$ at position *C*. At several points (marked *B* in Fig. 4) along the step edge, larger domains of $(\sqrt{3}\times\sqrt{3})$ are apparent. It can be seen that the original line of the step edge cuts these domains in half, and that the cavities in the upper terraces correspond to bulges in the lower terrace. This provides positive evidence that, at a monatomic step, growth of $(\sqrt{3}\times\sqrt{3})$ occurs perpendicular to the step edge in both directions, and that the proposed mechanism is valid. Although it is not described explicitly in the proposed mechanism, it should be noted that the growth dynamics require the elimination of the (7×7) stacking fault since this is not present in the $(\sqrt{3}\times\sqrt{3})$ structure formed.

In areas of higher coverage the number of $(\sqrt{3}\times\sqrt{3})$ regions growing at the step edge gradually increases, until the terraces in the neighborhood of the step are composed almost entirely of $(\sqrt{3}\times\sqrt{3})$ (Fig. 5). At this point we observe that there are two types of $(\sqrt{3}\times\sqrt{3})$ domain which, as in the lower part of Fig. 2(a), are at different heights. The upper region, or island, is approximately 4 Å above the dark region, or hole, within which the $(\sqrt{3}\times\sqrt{3})$ structure is also present. As indicated earlier, the ratio of the area of the hole to the area of the island, S_h/S_i, has been used by other workers[7,8] as an experimental test for the validity of proposed growth mechanisms. For the coverage illustrated by Fig. 5, this ratio $S_h/S_i=0.45\pm0.04$, is considerably less than 0.89, the value predicted by theory. This is in conflict with previous reports,[7,8] but is indicative of a step-mediated growth mechanism where the $(\sqrt{3}\times\sqrt{3})$ region, which has grown into the terrace, almost doubles the total area of the island domain. In the filled states scanning tunneling microscope images, dark lines are often observed at this coverage between adjacent $(\sqrt{3}\times\sqrt{3})$ domains. These lines correspond to antiphase boundaries (APB), similar to those found for growth of Ag on Si(111) (Ref. 13) and for growth of Au on Si(111).[10,11] The details of the atomic arrangement across such an APB will be discussed below. Often two neighboring domains come close to one another but do not touch, and in this case a cusp in the $(\sqrt{3}\times\sqrt{3})$ island is observed at the step edge, suggesting that the reaction mechanism is driven by a curved boundary between the two phases. As a result, the width of the band of $(\sqrt{3}\times\sqrt{3})$, which runs along the step edge, varies irregularly from zero up to about 250 Å in some cases.

At this point it is useful to identify a trend in the course of the reaction as a function of surface coverage. Ag atoms impinge on the (7×7) surface, lose energy to the surface, probably by phonon creation, but retain sufficient lateral energy at 450 °C to overcome the diffusion barrier, and thus move freely over the (7×7) terrace. It appears that the dilute mobile Ag atoms do not react readily with the atoms on the terrace and have a higher occupational probability at the step along which they can move freely. As a result, chemical attack occurs at some point along the kinked step, resulting in a preferred site for further attack by other Ag atoms. This accounts for the development of larger independent islands of $(\sqrt{3}\times\sqrt{3})$ at these points [Fig. 2(a)], as opposed to many small islands and a full frontal attack at the step

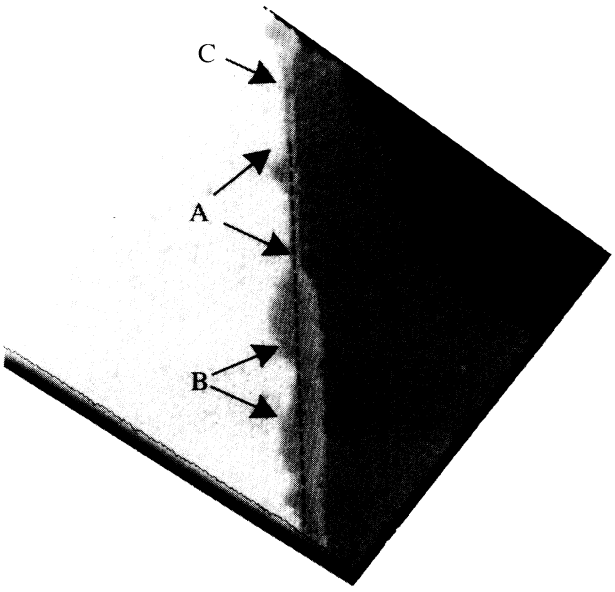

FIG. 4. Image of the early stages of growth at a monatomic step (600×600 Å^2, $I=1.1$ nA, $V=-0.8$ V). See text for explanation of symbols.

FIG. 5. Image of a step edge where the neighboring terrace is composed entirely of $(\sqrt{3}\times\sqrt{3})$. In addition to the island of $(\sqrt{3}\times\sqrt{3})$ along the edge of the step, the $(\sqrt{3}\times\sqrt{3})$ structure also exists within the low regions which appear dark in the image. (994×793 Å^2, $I=0.8$ nA, $V=-0.9$ V.)

edge. As the coverage of Ag atoms increases, the growth of islands elongates along the step direction at a greater rate than perpendicular to the step, resulting in a "saturated" $(\sqrt{3}\times\sqrt{3})$ step of a given depth. As the coverage is increased beyond the point where attack of Ag at the step edge has slowed, preferred reaction occurs on the (7×7) terrace in the vicinity of the $(\sqrt{3}\times\sqrt{3})$ step, as mentioned above, hence the appearance of holes as seen in Fig. 2(a) and Fig. 5. The reason for this change in reaction mode is not clear, but may be associated with the rate of diffusion of ejected silicon from the upper terrace, across $(\sqrt{3}\times\sqrt{3})$, to the reaction front on the lower terrace, i.e., the reaction stages are in this case balanced by the availability of mobile Si relative to the concentration of Ag atoms, which have a greater opportunity to react with the terrace. The confluence of steps can increase the local concentration of Ag atoms due to rebound from steps so that the reaction trend is subject to the local step density. Developments at still higher surface coverages will be described below.

B. Reaction on the terraces

At still higher densities of mobile atoms, the probability of attack of the (7×7) surface increases in regions of the terrace which are remote from the steps. As a result, so-called "hole-island" configurations arise where Si is ejected from the terrace and reacts with adsorbed Ag to yield islands at a level above the (7×7) adatoms [Fig. 6(a)]. The step height between the holes and the islands is approximately 4 Å, and these clearly correspond to the hole-island pairs which have been reported previously in the literature.[7,8] Both the hole and the island regions exhibit the $(\sqrt{3}\times\sqrt{3})$ structure, and we have no evidence to suggest any subtle differences in the structure of the two domains. The ratio of the area of the hole to the area of the island for this coverage has been measured as $S_h/S_i=1.01\pm0.09$, which is in reasonable agreement with the values previously reported in the literature. It can be seen that, with respect to the surrounding (7×7) surface, the Si trimers associated with the $(\sqrt{3}\times\sqrt{3})$ structure[6] are positioned at the H_3 sites in the hole region, whereas, on the island, the trimers lie over the T_4 sites [Fig. 6(b)], an observation which is also consistent with earlier studies.[5,7] Note that due to the range of heights in the original data, it was necessary to apply a band-pass filter to this image in order to show the detail in both the hole and the island regions. This results in some anomalies at the step edge; for this reason no emphasis is placed on the structure in this region.

A schematic diagram of the mechanism proposed for hole-island pair formation, based on that by Shibata and co-workers,[7,8] is shown in Fig. 7. It is proposed that Ag atoms diffuse across the terrace and react, at a suitable site (which cannot be identified), with the silicon atoms in the basal plane to form the $(\sqrt{3}\times\sqrt{3})$ structure at a level below that of the (7×7) surface. For reaction of one (7×7) unit cell, the formation of the silicon trimers associated with the $(\sqrt{3}\times\sqrt{3})$ structure would require only 50 of the 102 silicon atoms in a (7×7) unit cell. Thus, 52 silicon atoms are ejected onto the surrounding region of

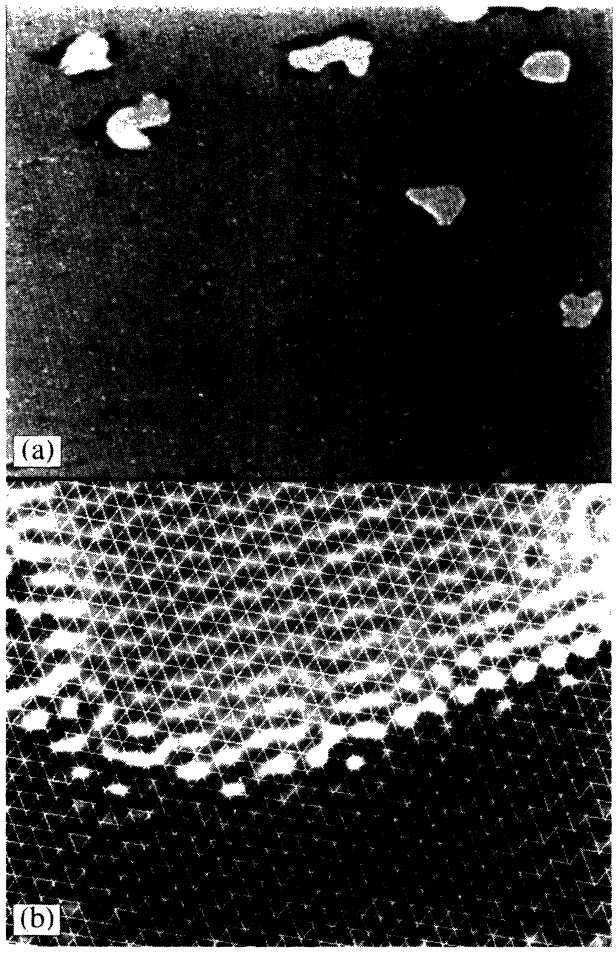

FIG. 6. (a) Image of isolated hole-island pairs on a Si(111)-(7×7) terrace. The $(\sqrt{3}\times\sqrt{3})$ structure is present both in the holes and on the islands. (2000×1140 Å^2, $I=0.8$ nA, $V=-0.9$ V.) (b) Magnified image of a hole-island pair, displayed as a differential image. The triangular mesh of the Si (1×1) structure indicates the position of the T_4 sites. The dark minima on the island, which correspond to the silicon trimers, are at the T_4 sites, whereas in the hole region they align with the H_3 sites.

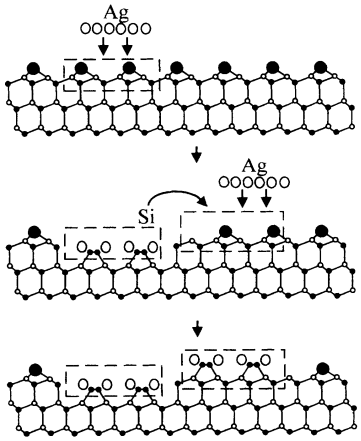

FIG. 7. Schematic diagram of the proposed mechanism for hole-island pair formation. The atom representations are as given in Fig. 3.

(7×7) where they can undergo reaction with additional Ag atoms. In order to form the $(\sqrt{3}\times\sqrt{3})$ structure at a level above that of the $(\sqrt{3}\times\sqrt{3})$ in the hole region, an area of (7×7) must first be unreconstructed to a defect-free bilayer, as found on a Si(111)-(1×1) surface. This requires extensive rearrangement of the (7×7) surface, and, for one unit cell, consumes 98 of the 102 Si atoms available. Therefore, the total number of silicon atoms available to form silicon trimers in the island domain of $(\sqrt{3}\times\sqrt{3})$ is 56, i.e., 52+4. As a result, the $(\sqrt{3}\times\sqrt{3})$ island domain will be larger than one (7×7) unit cell, and the actual number of Si atoms involved will be slightly larger than 56 since an additional area of (7×7) must be rearranged.

From the scanning tunneling microscope images alone, we cannot deduce for certain whether or not the $(\sqrt{3}\times\sqrt{3})$ structure in the hole extends underneath the $(\sqrt{3}\times\sqrt{3})$ island. The mechanism proposed above suggests that this is not the case; a perfect silicon bilayer should be found directly below the $(\sqrt{3}\times\sqrt{3})$ layer. Experimental evidence to support this comes from investigation of antiphase boundaries on some $(\sqrt{3}\times\sqrt{3})$ islands [Fig. 8(a)]. Following the line of the APB into the $(\sqrt{3}\times\sqrt{3})$ hole, it can be seen that there is no corresponding boundary in the lower domain. If the APB was present in both domains, and aligned across the upper and lower $(\sqrt{3}\times\sqrt{3})$ domains, it would suggest that the upper terrace was $(\sqrt{3}\times\sqrt{3})$ growing on $(\sqrt{3}\times\sqrt{3})$. Since this is not the case, i.e., the APB does not align across the step, and conversely APB's in hole regions do not extend into islands, it suggests that a silicon bilayer is present below both domains.

C. Structure of the antiphase boundary

Figure 8(b) shows in detail the area around an APB. A band-pass filter was applied to this image to enhance the $(\sqrt{3}\times\sqrt{3})$ structure for presentation purposes; however, one negative effect of this is an increase in the brightness of the boundary with respect to the surrounding structure. The APB is aligned along the $[11\bar{2}]$ direction, and has a Burgers vector in the $[10\bar{1}]$ direction with a magnitude of approximately 3.6 Å. The size and direction of the Burgers vector indicate that the silicon trimers on either side of the APB have been displaced between adjacent T_4 sites in the underlying bilayer, which would correspond to a Burgers vector of magnitude 3.8 Å.

The overlay (1×1) mesh in Fig. 8(b) shows the position of the T_4 sites, aligned with the $(\sqrt{3}\times\sqrt{3})$ domain by referencing to the surrounding (7×7) surface. This grid clearly illustrates that the silicon trimers, which correspond to the minima in the image, are positioned over the T_4 sites on both sides of the boundary. Several APB's have been analyzed, and all of the results indicate that the silicon trimers of the $(\sqrt{3}\times\sqrt{3})$ structure are located on the same type of site on each side of the boundary. As noted earlier, in the lower, or hole regions of $(\sqrt{3}\times\sqrt{3})$, the silicon trimers are positioned at the H_3 sites with respect to the surrounding (7×7) surface, and, consequently, the silicon trimers also align with the H_3 sties on each side of APB's in these regions. This is the

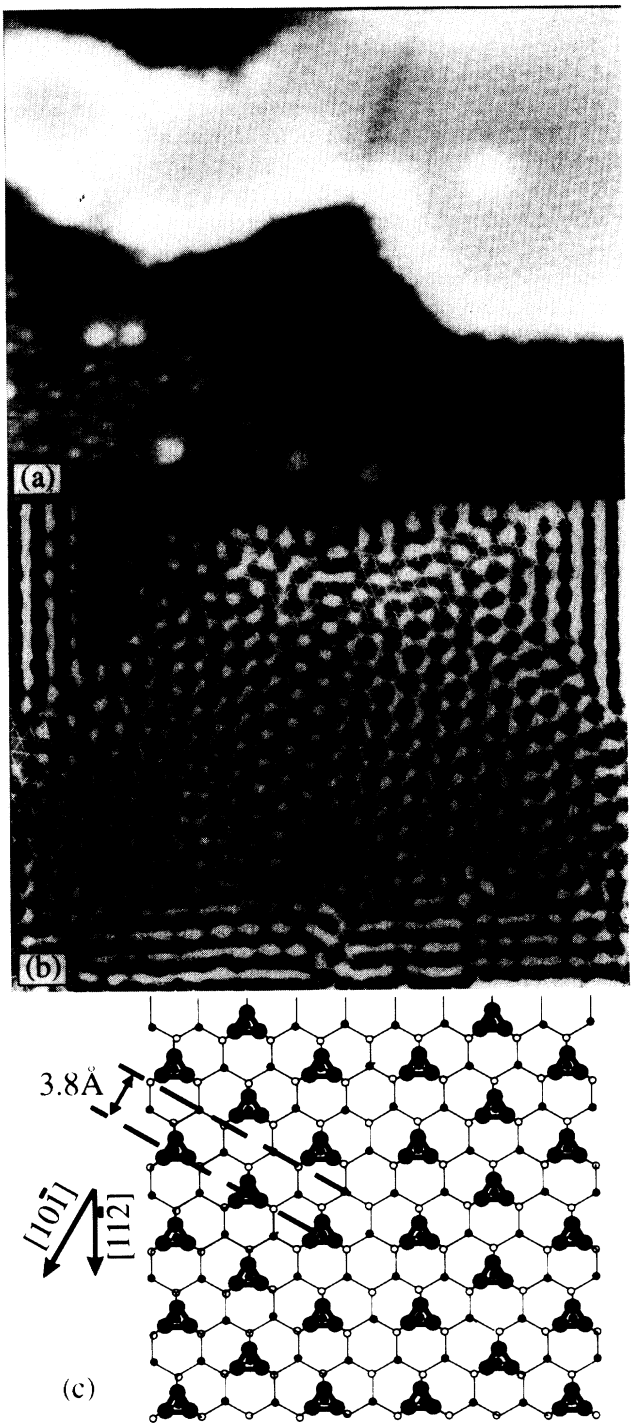

FIG. 8. (a) Image of an island in which an APB is present. Note that the APB does not continue into the hole region. (427×340 Å^2, $I=0.8$ nA, $V=-0.9$ V.) (b) Expanded region of (a) showing the detailed structure in the region of the APB. The triangular grid indicates the T_4 sites of a Si (1×1) structure. Clearly, the silicon trimers are positioned at the T_4 sites on both sides of the boundary. (c) Schematic diagram showing the structure in the vicinity of the APB. For clarity, only the silicon trimers of the $(\sqrt{3}\times\sqrt{3})$ structure are shown on a (1×1) lattice. The Burgers vector associated with the displacement across the boundary is in the $[10\bar{1}]$ direction, with a measured magnitude of 3.6 Å (compared with predicted value of 3.8 Å).

case for the APB indicated in Fig. 10(b) below. Shown in Fig. 8(c) is a schematic showing the arrangement of the Si trimers across the APB shown in Fig. 8(b). This shows that while the trimers are centered over T_4 sites on either side of the boundary, there may be a region at the center of the APB which exhibits a (1×1) structure.

It might be suggested that these APB's are associated with domain boundaries on the (7×7) surface. This can be discounted for a number of reasons. First, the domain size on the (7×7) surface is much larger (>5000 Å) than the size of the $(\sqrt{3}\times\sqrt{3})$ domains. Second, domain boundaries on the (7×7) surface generally extend a considerable distance, and are terminated at step edges or defects. If the APB's on the $(\sqrt{3}\times\sqrt{3})$ were associated with such a defect, we would expect to observe a number of APB's closely spaced and aligned in the same general direction, which is not the case. Finally, such domain boundaries on the (7×7) surface are often observed to terminate at a monatomic step. This implies that the defect is formed by misalignment of the adatom and rest-atom layers of adjacent regions. If this is indeed the case, then since the formation of the $(\sqrt{3}\times\sqrt{3})$ structure requires the elimination of the (7×7) stacking fault, the (7×7) domain boundaries would also be removed.

The conclusions reached regarding the structure of the APB are significantly different from the results obtained by Wan, Lin, and Nogami,[13] who report that the silicon trimers are at T_4 sites on one side of the boundary and at H_3 sites on the other side. In this work the $(\sqrt{3}\times\sqrt{3})$ surface was formed by deposition of Ag onto a hot substrate, whereas in the study by Wan, Lin, and Nogami,[13] the sample was formed by deposition onto a cold Si(111) wafer with subsequent annealing. Previous STM studies have assumed, or implied, that the $(\sqrt{3}\times\sqrt{3})$ surfaces prepared by these two methods are identical.[5,7] However, the results described above and those reported by Wan, Lin, and Nogami[13] indicate that the atomic arrangement across an APB, and consequently the structure of individual $(\sqrt{3}\times\sqrt{3})$ domains, are sensitive to the preparation method.

FIG. 9. Hole-island pairs interacting on a terrace. Note a number of small dark holes and bright dots on the terrace. Also apparent is the presence of ridges around the edges of the islands (1547×1234 Å^2, $I=0.8$ nA, $V=-0.9$ V).

D. Interaction of the hole-island pairs

As the concentration of mobile Ag atoms increases further, the number and size of hole-island pairs observed on the silicon terraces increases (Fig. 9). The hole-island ratio measured at this coverage is significantly smaller, $S_h/S_i=0.56\pm0.12$, than that measured for lower cover-

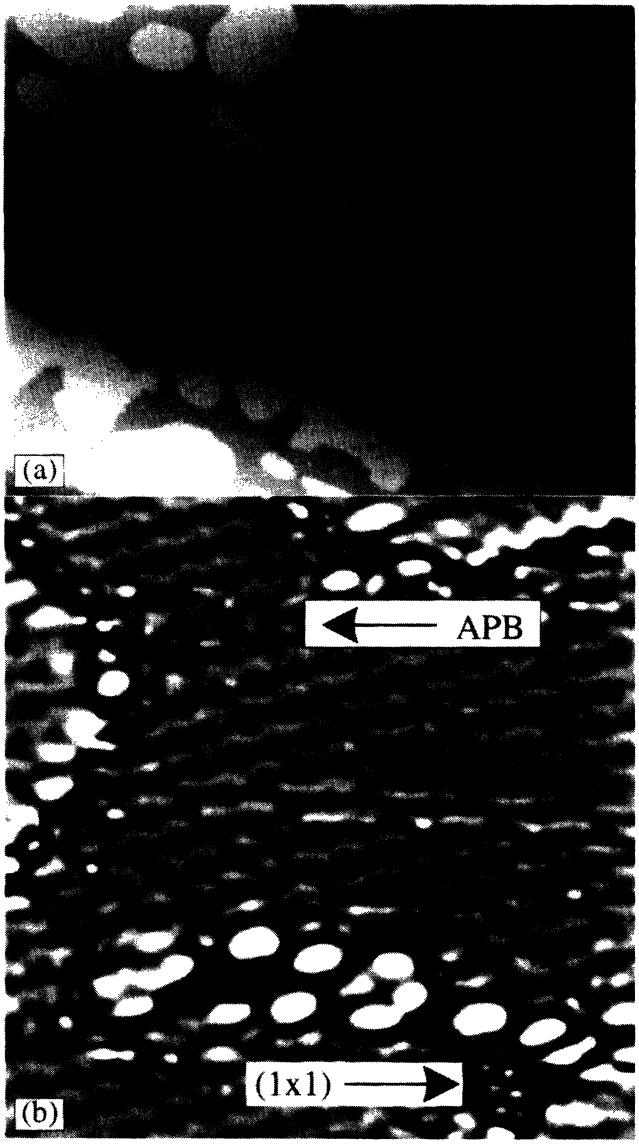

FIG. 10. (a) Image of the Ag/Si(111)-$(\sqrt{3}\times\sqrt{3})$ surface at close to monolayer coverage. The surface essentially consists of $(\sqrt{3}\times\sqrt{3})$ islands and $(\sqrt{3}\times\sqrt{3})$ terraces. However, a number of disordered regions are also apparent (2000×1600 Å^2, $I=1.1$ nA, $V=-1.1$ V). (b) Expanded section of a disordered region displayed as a differential image. The surrounding regions of $(\sqrt{3}\times\sqrt{3})$ are apparent, and in the center of these a small area which exhibits the Si(111)-(1×1) structure is observed.

ages where the hole-island pairs are isolated from each other on a silicon terrace. The hole-island pairs may grow into one another, and antiphase boundaries, identical to those found between domains at the step edges, are sometimes observed at the meeting point of two $(\sqrt{3}\times\sqrt{3})$ domains.

Close study of the images at this coverage reveals a number of small black holes and bright spots in the filled-states images (Fig. 9). These regions are usually a fraction of a (7×7) unit cell in size. The measured depth of the holes implies that the $(\sqrt{3}\times\sqrt{3})$ structure may be present at the bottom of the hole, but in the majority of cases this cannot be resolved by STM. If this is the case, it is reasonable to assume that the bright spots are due to silicon atoms, which have been ejected from the hole region but have not reacted with Ag atoms, possibly due to insufficient concentration of mobile Ag atoms. We discount the possibility that the bright spots are due to adsorbed hydrogen atoms since they are not observed in regions of lower Ag coverage. On this basis, it is postulated that growth of hole-island pairs begins via nucleation of $(\sqrt{3}\times\sqrt{3})$ at a large number of sites on a (7×7) terrace, but continues only at a few of these sites at the expense of others. The orientation of the hole with respect to the island appears to vary considerably. It is possible that the shape of the hole is determined by the position of other nucleation sites on the surface. It is interesting to note that in some cases peninsulas of (7×7), as small as one or two unit cells, are observed, which remain stable despite being completely surrounded by the $(\sqrt{3}\times\sqrt{3})$ structure. This is a clear indication of the very-short-range nature of the bonding in the (7×7) structure.

In the images of the hole-island pairs a ridge is present around the edge of each island. This ridge, which is typically 0.5–1 Å above the $(\sqrt{3}\times\sqrt{3})$ structure of the island, is not continuous around the edge of the island but is present in almost every image. A similar feature is seldom observed around the edge of a hole domain where it borders the (7×7) surface. The position at which the ridge occurs has a complex structure, being the meeting between two $(\sqrt{3}\times\sqrt{3})$ domains, the hole, and the island, as well as with the silicon layer beneath the $(\sqrt{3}\times\sqrt{3})$ island domain. This leads to the postulate that the ridge could be due to strain effects.

E. Investigation of monolayer coverages and beyond

As the coverage increases and the distance between neighboring $(\sqrt{3}\times\sqrt{3})$ domains becomes small, highly disordered regions are apparent between some domains [Fig. 10(a)]. The area of these regions varies widely, and in the smaller regions a more ordered structure is observed [Fig. 10(b)]. A band-pass filter, optimized to enhance the latter structure as well as the $(\sqrt{3}\times\sqrt{3})$ regions, was applied to this image to reduce the dynamic range for display purposes This structure is identified as a Si(111)-(1×1) surface with a measured unit cell dimension of 3.6 Å, in reasonable agreement with the theoretical value 3.84 Å. It is believed that this may be the first time such a structure has been imaged at room temperature with atomic resolution using STM. The regular (1×1) structure is only observed in regions which are less than about six unit cells in width. This suggests that larger regions of (1×1) are unstable, and, beyond a certain size, a disordered (1×1) phase results. As the width of the region between the $(\sqrt{3}\times\sqrt{3})$ domains decreases to about a single (1×1) unit cell, the region can be recognized as an APB, although presumably many regions become in-phase boundaries which cannot be observed by STM. A large number of antiphase boundaries can be identified on the $(\sqrt{3}\times\sqrt{3})$ terraces, formed by the joining up of the holes, and the existence of the (1×1) structure described above supports the proposed model of these APB's [Fig. 8(c)], which shows a band of (1×1) along the length of the boundary. At close to monolayer coverage, i.e., complete $(\sqrt{3}\times\sqrt{3})$ but showing no excess Ag, there is no evidence for the (7×7) structure, and the surface is now entirely $(\sqrt{3}\times\sqrt{3})$ islands on a $(\sqrt{3}\times\sqrt{3})$ terrace (Fig. 11). The hole-island ratio S_h/S_i, obtained by measuring the area of $(\sqrt{3}\times\sqrt{3})$ islands on the $(\sqrt{3}\times\sqrt{3})$ terrace, was measured to be 0.78 ± 0.05, which is less than that found for isolated hole-island pairs.

When the coverage is increased significantly beyond a monolayer by deposition of more Ag onto the sample, the surface is found to be comprised of a number of platelets. These platelets are flat on top, and have edges which are aligned along the $\langle 110\rangle$ crystallographic directions. Although atomic resolution images of the surface of these platelets could not be obtained, the evidence suggests that these are islands of Ag(111) which have grown epitaxially on the $(\sqrt{3}\times\sqrt{3})$ structure. This is consistent with observation by Demuth *et al.*[2] for deposition of 5.8 ML (monolayer) of Ag on Si(111)-(7×7). Since growth of (111) platelets of silver is observed at high coverage, it can be concluded that the formation of the $(\sqrt{3}\times\sqrt{3})$ structure is a self-terminating reaction. Thus, returning to the question of whether or not the $(\sqrt{3}\times\sqrt{3})$ domain in a hole extends beneath the $(\sqrt{3}\times\sqrt{3})$ island, it is concluded that there is a silicon layer directly beneath each $(\sqrt{3}\times\sqrt{3})$ domain regardless of whether it is a hole region or an island.

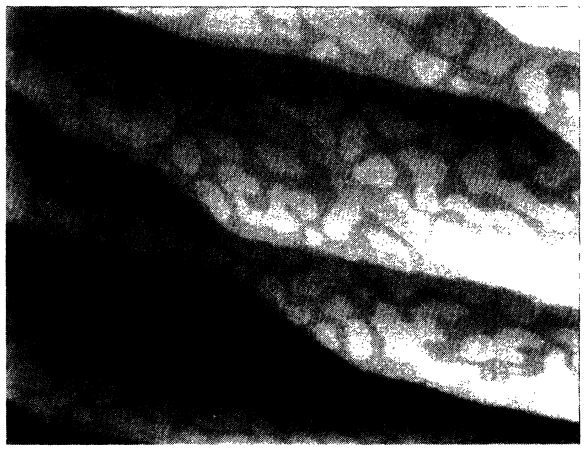

FIG. 11. Image of the Ag/Si(111)-$(\sqrt{3}\times\sqrt{3})$ at full monolayer coverage. There is little evidence at this coverage of large regions of disorder. (2000×1600 Å^2, $I=1.1$ nA, $V=-2.4$ V.)

The results clearly show that the location of the $(\sqrt{3}\times\sqrt{3})$ domains on the Si surface is dependent on the coverage. At the lowest coverage, isolated $(\sqrt{3}\times\sqrt{3})$ domains grow at step edges. Once the number and size of these domains has increased to the point where a step edge has a band of $(\sqrt{3}\times\sqrt{3})$ along its length, holes which also contain the $(\sqrt{3}\times\sqrt{3})$ structure develop adjacent to the $(\sqrt{3}\times\sqrt{3})$ band. When all available sites at a step edge have reacted, a transition to growth on the terraces occurs, where isolated hole-island paris are formed. This mode of growth continues until the entire terrace is made up of the $(\sqrt{3}\times\sqrt{3})$ structure. Further deposition of Ag results in the growth of three-dimensional islands of Ag, which almost certainly have the (1×1) structure of the Ag(111) surface. The transition from growth at the step edge to growth on the terraces can be visualized as a saturation of the high-energy sites at the step edges followed by reaction at the lower-energy sites on the terraces. This implies that initial nucleation on the terraces will occur at the most reactive sites, possibly those associated with defects. The coverage at which the transition between growth at the step edge and growth on the terraces occurs is dependent on the local step density, which can vary considerably on the Si(111)-(7×7) surface, especially after desorption of Ag. The dependence on local step density makes it extremely difficult to quote a specific value for the coverage at which the transition occurs. In addition, the transition between the growth mode is unlikely to be abrupt, due to the influence of the step density and the local geometry of the surface. However, for the image shown in Fig. 2(a), which is typical of those acquired, it can be estimated that the total coverage of $(\sqrt{3}\times\sqrt{3})$ is about 6%, but in the triangular region at the confluence of the steps it increases to abut 30% of the surface.

F. Area ratio of hole to island

The final point for discussion is the ratio of the area of the hole to that of the island, which contrary to the results of other workers,[7,8,13] we do not find to be constant as a function of Ag coverage. This ratio varies from zero for the lowest coverage, where the $(\sqrt{3}\times\sqrt{3})$ domains have no associated hole region, to about 0.45 when holes develop at the step edges, and approximately unity for coverages where isolated hole-island pairs exist on the terraces. The measured ratio decreases to about 0.6 for coverages where interaction of the hole-island pairs occurs, and appears to reach a plateau value of about 0.8 for complete $(\sqrt{3}\times\sqrt{3})$ coverage. This variation is illustrated in Fig. 12, but it should be noted that the values used on the abscissa are very approximate. The ratios were obtained from the scanning tunneling microscope images by measuring the number of data points which were above and below a threshold level, which was set relative to the plane of the (7×7) surface. A relationship between the hole-island ratio and the number density of silicon atoms in the $(\sqrt{3}\times\sqrt{3})$, $N_{\sqrt{3}}$, and (7×7) N_7 structures, can be derived by assuming conservation of the number of silicon atoms in the transition from (7×7) to $(\sqrt{3}\times\sqrt{3})$. On this basis we obtain

$$\frac{S_h}{S_i}=\frac{2}{N_7-N_{\sqrt{3}}}-1\ .$$

This expression, identical to that derived by Shibata, Kimura, and Takayanagi,[7] can be used to predict a value for S_h/S_i by taking $N_7=2.08$ ML, assuming the dimer-adatom-stacking fault (DAS) model[12] for (7×7), and $N_{\sqrt{3}}=1.02$ ML, assuming the HCT model[4] for $(\sqrt{3}\times\sqrt{3})$ (1 ML$=7.84\times10^{14}$ atoms/cm^2). The theoretical result is $S_h/S_i=0.89$, which is in good agreement with the values measured at coverages where isolated hole-island pairs are found on the terraces. The deviation of S_h/S_i away from the theoretical value at higher coverage is not understood. At low coverage it has been shown that growth occurs at the step edge, resulting in a band of $(\sqrt{3}\times\sqrt{3})$ along the edge before any formation of hole-island pairs occurs. Since there is no demarcation between the initial band of $(\sqrt{3}\times\sqrt{3})$ formed and the upper domain of the hole-island growth, which occurs subsequently at the step edge, the ratio measured is considerably less than unity. It is interesting to speculate that if half of the island area at the step edge was formed by the mechanisms outlined in Fig. 3, while half was formed by growth of hole-island pairs at the step edge, S_h/S_i for the second growth stage would be in the range 0.9–1.0.

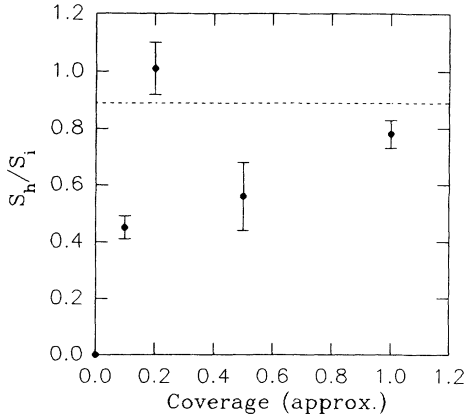

FIG. 12. Plot of the ratio of the area of a hole to the area of an island, S_h/S_i, as a function of Ag coverage. The dashed horizontal line indicates the theoretical value for S_h/S_i, based on the proposed mechanism for hole-island pair formation. The deviation from the theoretical value at low coverages ($\theta<0.2$) is due to step-mediated growth mechanics. At higher coverages ($\theta>0.5$) the origin of the discrepancy is unclear.

IV. SUMMARY

In summary, the reaction of Ag with Si(111)-(7×7) has been studied at 450 °C. It is observed that the different arrangements of the resulting $(\sqrt{3}\times\sqrt{3})$ phase depend upon the surface density of Ag atoms. The local density of Ag atoms is modified by the step density, such that several phases are seen at any time. The mobility of ejected Si atoms over the $(\sqrt{3}\times\sqrt{3})$ phase is also

thought to influence a transition from step growth to a terrace etching process. At higher surface densities of Ag, hole-island pairs appear, which finally coalesce to larger areas. Prior to full coverage, and as the $(\sqrt{3}\times\sqrt{3})$ domains begin to grow into each other, different gaps between the domains lead to (a) large disordered regions of Si, (b) smaller openings where Si(111)-(1×1) appears to be stable, and (c) antiphase boundaries where mismatch between domains occurs. The atomic arrangement across antiphase boundaries has been investigated; a structural model is proposed that is consistent with our observation that the silicon trimers of the $(\sqrt{3}\times\sqrt{3})$ structure are positioned over the same site on each side of the boundary.

[1]R. J. Wilson and S. Chaing, Phys. Rev. Lett. **58**, 369 (1987).
[2]J. E. Demuth, E. J. van Loenen, R. M. Tromp, and R. J. Hamers, J. Vac. Sci. Technol. B **6**, 18 (1988).
[3]E. J. van Loenen, J. E. Demuth, R. M. Tromp, and R. J. Hamers, Phys. Rev. Lett. **58**, 373 (1987).
[4]T. Takahashi and S. Nakatani, Surf. Sci. **282**, 17 (1993).
[5]K. J. Wan, X. F. Lin, and J. Nogami, Phys. Rev. B **45**, 9509 (1992).
[6]M. Katayama, R. S. Williams, M. Kato, E. Nomura, and M. Aono, Phys. Rev. Lett. **66**, 2762 (1991).
[7]A. Shibata, Y. Kimura, and K. Takayanagi, Surf. Sci. Lett. **275**, L967 (1992).
[8]A. Shibata and K. Takayanagi, Jpn. J. Appl. Phys. **32**, 1385 (1993).
[9]Omicron Vakuumphysik, Germany.
[10]T. Hasegawa, K. Takata, S. Hosaka, and S. Hosoki, J. Vac. Sci. Technol. A **8**, 241 (1990).
[11]J. Nogami, A. A. Baski, and C. F. Quate, Phys. Rev. Lett. **65**, 1611 (1990).
[12]K. Takayanagi, Y. Tanishiro, S. Takahashi, and M. Takahashi, Surf. Sci. **164**, 367 (1985).
[13]K. J. Wan, X. F. Lin, and J. Nogami, Phys. Rev. B **47**, 13 700 (1993).
[14]J. A. Venables, Phys. Rev. B **36**, 4153 (1987).
[15]R. M. Feenstra and M. A. Lutz, Phys. Rev. B **42**, 5391 (1990).

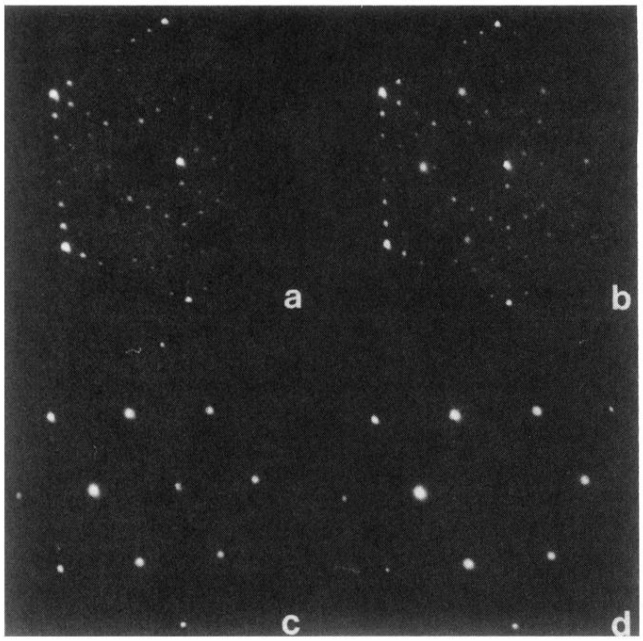

FIG. 1. LEED patterns showing an Ag $(\sqrt{3}\times\sqrt{3})$ concentration gradient on Si(111). The diffraction patterns were recorded with a beam energy of 38 eV. Patterns recorded at the left-hand side of the crystal, (a), only show spots associated with Si(111)-(7×7). As the sample is traversed, (b) and (c), the intensity of the spots due to the $(\sqrt{3}\times\sqrt{3})$ structure increases, until at the right-hand side, (d), only the diffraction pattern due to $(\sqrt{3}\times\sqrt{3})$ is apparent.

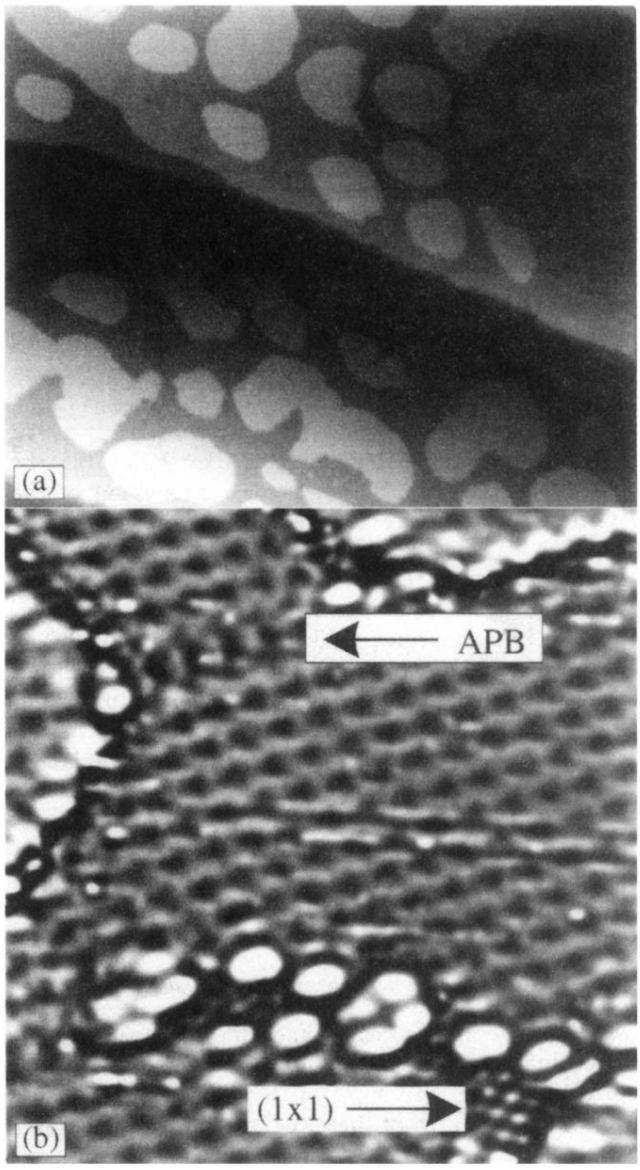

FIG. 10. (a) Image of the Ag/Si(111)-($\sqrt{3}\times\sqrt{3}$) surface at close to monolayer coverage. The surface essentially consists of ($\sqrt{3}\times\sqrt{3}$) islands and ($\sqrt{3}\times\sqrt{3}$) terraces. However, a number of disordered regions are also apparent (2000×1600 Å^2, $I=1.1$ nA, $V=-1.1$ V). (b) Expanded section of a disordered region displayed as a differential image. The surrounding regions of ($\sqrt{3}\times\sqrt{3}$) are apparent, and in the center of these a small area which exhibits the Si(111)-(1×1) structure is observed.

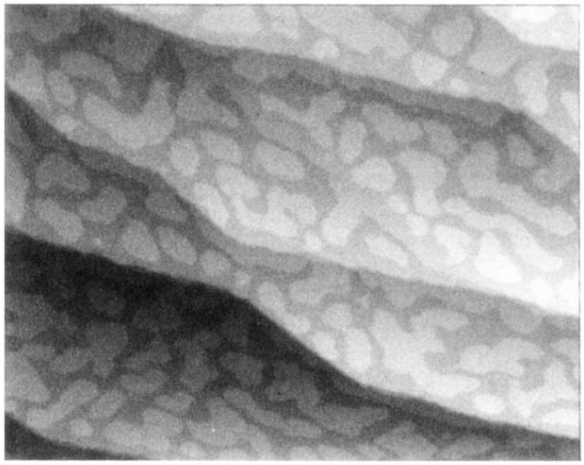

FIG. 11. Image of the Ag/Si(111)-($\sqrt{3}\times\sqrt{3}$) at full monolayer coverage. There is little evidence at this coverage of large regions of disorder. (2000×1600 Å^2, $I=1.1$ nA, $V=-2.4$ V.)

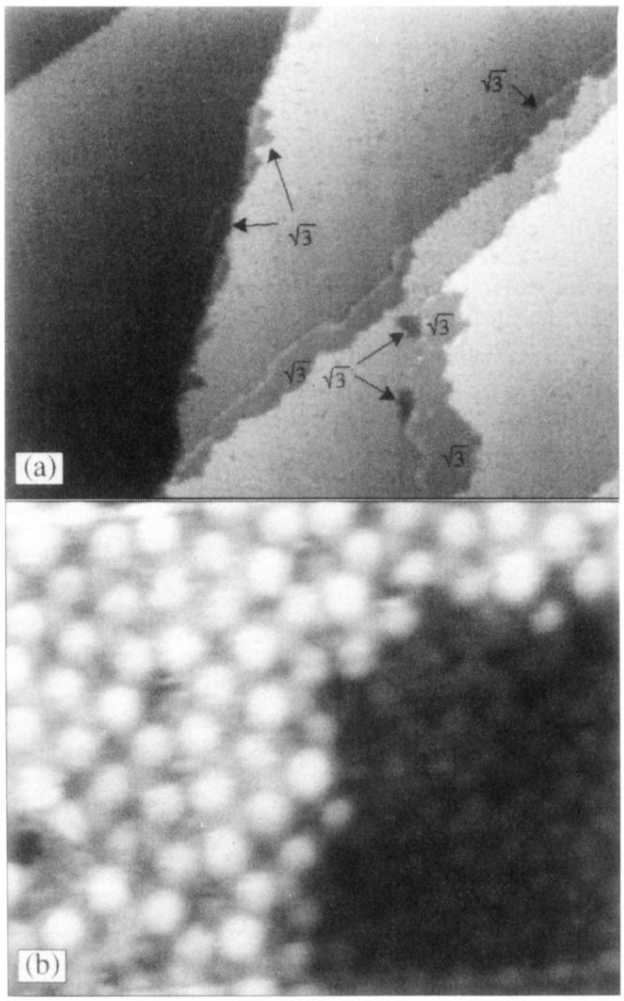

FIG. 2. (a) Image of the initial growth stage of Ag on Si(111) (1590×1270 Å^2, $I=1.2$ nA, $V=-0.9$ V). Isolated domains and bands of ($\sqrt{3}\times\sqrt{3}$) are apparent at the step edges. (b) Enlarged image of the interface between (7×7) and ($\sqrt{3}\times\sqrt{3}$).

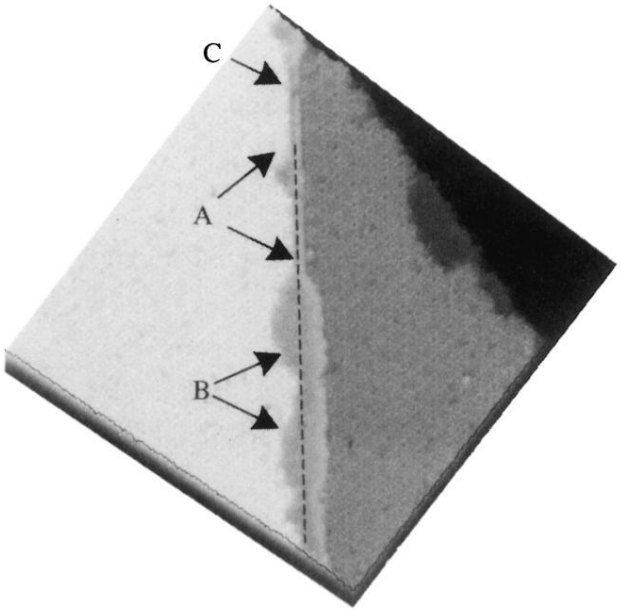

FIG. 4. Image of the early stages of growth at a monatomic step (600×600 Å^2, $I = 1.1$ nA, $V = -0.8$ V). See text for explanation of symbols.

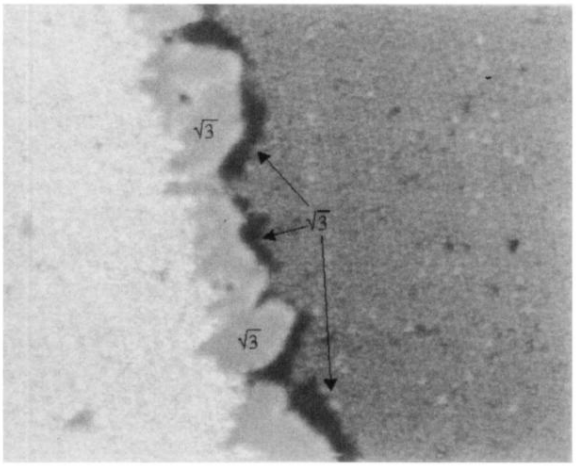

FIG. 5. Image of a step edge where the neighboring terrace is composed entirely of $(\sqrt{3}\times\sqrt{3})$. In addition to the island of $(\sqrt{3}\times\sqrt{3})$ along the edge of the step, the $(\sqrt{3}\times\sqrt{3})$ structure also exists within the low regions which appear dark in the image. (994×793 Å^2, $I=0.8$ nA, $V=-0.9$ V.)

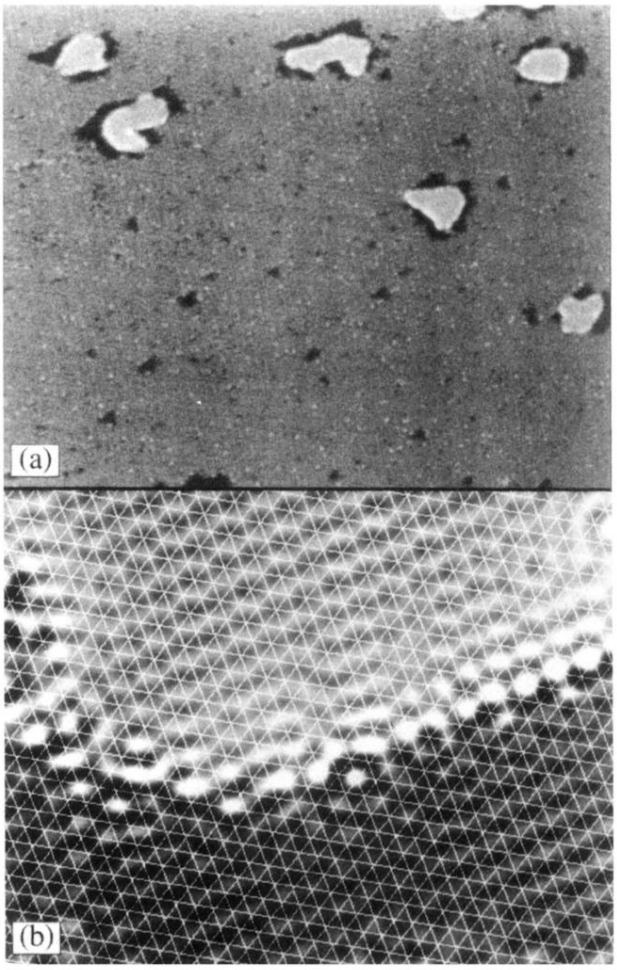

FIG. 6. (a) Image of isolated hole-island pairs on a Si(111)-(7×7) terrace. The $(\sqrt{3}\times\sqrt{3})$ structure is present both in the holes and on the islands. (2000×1140 Å^2, $I=0.8$ nA, $V=-0.9$ V.) (b) Magnified image of a hole-island pair, displayed as a differential image. The triangular mesh of the Si (1×1) structure indicates the position of the T_4 sites. The dark minima on the island, which correspond to the silicon trimers, are at the T_4 sites, whereas in the hole region they align with the H_3 sites.

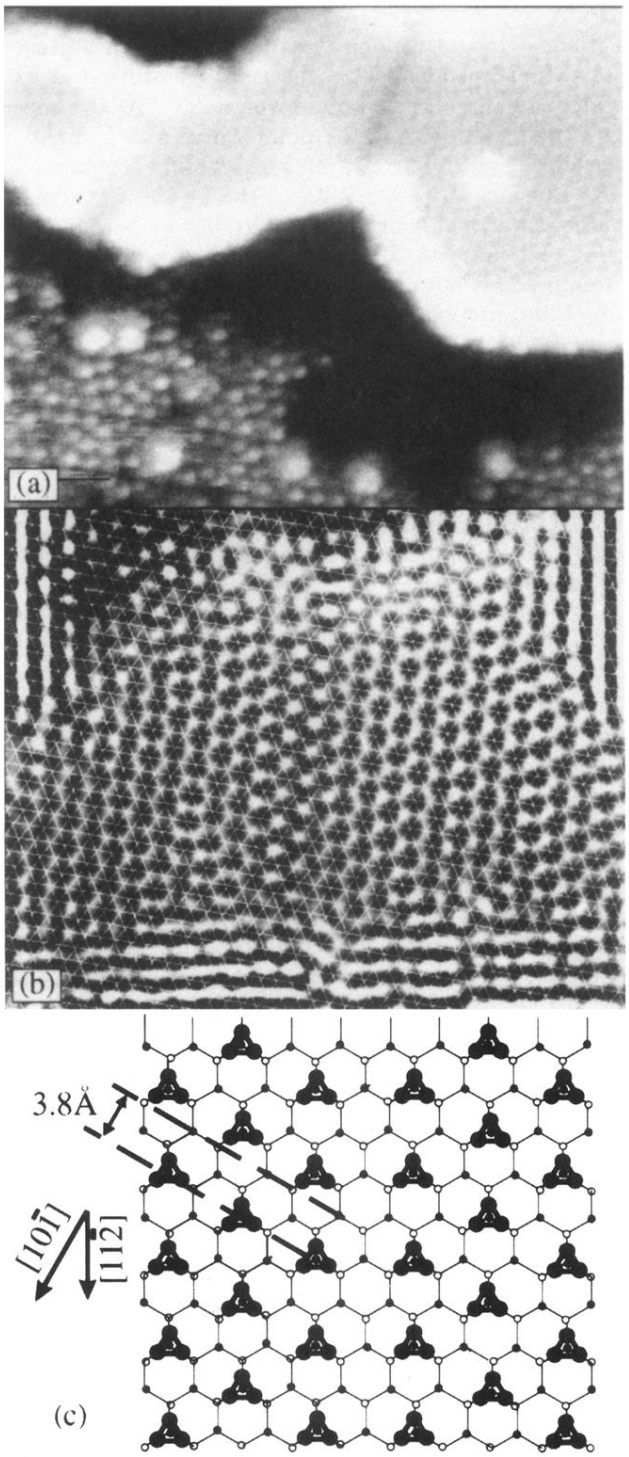

FIG. 8. (a) Image of an island in which an APB is present. Note that the APB does not continue into the hole region. (427×340 Å^2, $I=0.8$ nA, $V=-0.9$ V.) (b) Expanded region of (a) showing the detailed structure in the region of the APB. The triangular grid indicates the T_4 sites of a Si (1×1) structure. Clearly, the silicon trimers are positioned at the T_4 sites on both sides of the boundary. (c) Schematic diagram showing the structure in the vicinity of the APB. For clarity, only the silicon trimers of the $(\sqrt{3}\times\sqrt{3})$ structure are shown on a (1×1) lattice. The Burgers vector associated with the displacement across the boundary is in the $[10\bar{1}]$ direction, with a measured magnitude of 3.6 Å (compared with predicted value of 3.8 Å).

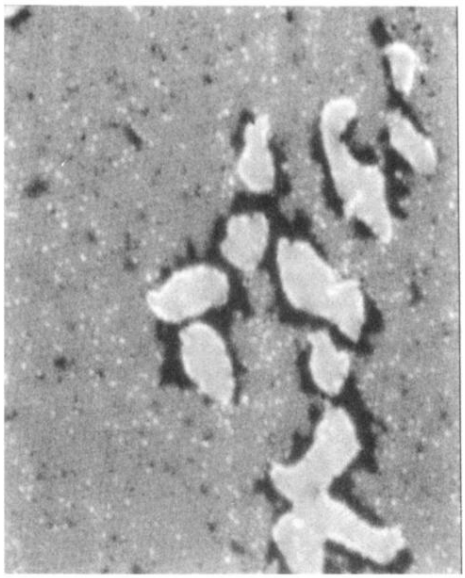

FIG. 9. Hole-island pairs interacting on a terrace. Note a number of small dark holes and bright dots on the terrace. Also apparent is the presence of ridges around the edges of the islands (1547×1234 Å^2, $I=0.8$ nA, $V=-0.9$ V).